Int J Legal Med (2011) 125:617–628
DOI 10.1007/s00414-010-0462-4

ORIGINAL ARTICLE

The effect of firearm muzzle gases on the backspatter of blood

Michael C. Taylor · Terry L. Laber · Barton P. Epstein · Dan S. Zamzow · David P. Baldwin

Received: 30 October 2009 / Accepted: 19 April 2010 / Published online: 12 May 2010

Abstract Injuries caused by gunshots can produce what bloodstain pattern analysts know as "backspatter." Observations about the presence or absence of backspatter on an individual may be used in court as evidence of guilt or innocence. The discharge of three firearms (.22 caliber revolver, .38 caliber revolver, and .308 caliber rifle) and the resulting impact of bullets on a blood source were recorded using high-speed digital video imaging. Blood droplets, firearm muzzle gases, and ballistic shock waves were visualized using standard reflected light and shadowgraphy imaging techniques. A significant interaction between air currents, muzzle gases, and particulate material emanating from the firearms upon discharge with backspattered blood was observed. Blood droplets, initially spattered back toward the firearm and the shooter, were observed to change direction under the influence of firearm-induced air currents and were blown forward toward and beyond their original source location. Implications for experts testifying in court and for bloodstain pattern instructors are discussed.

M. C. Taylor (✉)
Institute of Environmental Science and Research Limited (ESR),
P O Box 29-181, Christchurch, New Zealand
e-mail: michael.taylor@esr.cri.nz

T. L. Laber
Minnesota Bureau of Criminal Apprehension (BCA),
1430 Maryland Ave East,
St. Paul, MN 55106, USA

B. P. Epstein
4520 Sedum Lane,
Edina, MN 55435, USA

D. S. Zamzow · D. P. Baldwin
Midwest Forensics Resource Center, Ames Laboratory-USDOE,
Iowa State University,
Ames, IA 50011, USA

Keywords Backspatter · Shadowgraphy · Bloodstain pattern · Gunshot · High-speed video

Introduction

It is well known that when a gunshot wound is inflicted, blood and tissue can be projected back toward the firearm and the shooter. This has become known to bloodstain pattern analysts as "backspatter." The presence of backspatter on a firearm or on the shooter has been used to draw inferences about the proximity of the shooter to the intended target [1–3].

In basic bloodstain pattern courses, students are taught to recognize bloodstain patterns from firearm-induced blood events. A typical experiment or demonstration involves the use of a blood-soaked sponge suspended between cardboard targets set at varying distances from the sponge [4]. The firearm is discharged and the bullet passes through the first target through the bloodied sponge and exits through the second target. Both targets are bloodstained. The pattern on the first target is used to illustrate backspatter and that on the second target shows the "forward spatter."

In a recently completed project [5] aimed at capturing a number of blood-letting events on video, the authors became aware of a phenomenon that has not yet been reported in the literature and which is a factor that hitherto may not have been taken into account by those seeking to interpret the presence or absence of bloodstains in firearm-related incidents. This phenomenon is the interaction between gases released during the discharge of a firearm and blood drops generated by the impact of the bullet on a liquid blood source. Although the principles of firearm ballistics are generally well known, the impact of ballistic shock waves and firearm muzzle gases on any induced blood backspatter has not been previously investigated.

In this paper, we describe our observations of the spattering of blood from the impact of a bullet on a blood source and the effect of firearm-induced air currents on this spatter.

Materials and methods

The study was conducted in two parts. In the first part, the discharge of several firearms was studied using high-speed digital video imaging. The various stages of the discharge were recorded. These included the production of ballistic shock waves, the emergence of pressurized gases, and the projection of the bullet itself. In the second part of the study, the impact of a bullet on a source of liquid blood, along with the associated interaction of ballistic shock waves and muzzle gases, was recorded with high-speed digital video imaging. All firearm experiments were conducted in the firing range of the Minnesota Bureau of Criminal Apprehension

Three firearm/ammunition combinations were used:

- .22 Long Rifle caliber revolver with Federal .22 Long Rifle high-velocity ammunition (40 grain solid copper-plated bullet) or CCI Blazer .22 Long Rifle ammunition (40 grain lead bullet);
- .357 Magnum caliber Colt Trooper Mark 3 revolver, with Federal American Eagle .38 Special ammunition (AE38K, 130 grain full metal jacketed bullet); and
- .308 Winchester caliber Browning model 81 rifle with Remington Core-Lokt .308 Winchester ammunition (150 grain Core-lokt pointed soft point bullet).

Two imaging techniques were used. The first was direct lighting of the subject using two ellipsoid beam theater lights with 750-W tungsten lamps and two 1,000-W quartz tungsten halogen lamps (PhotonBeam 1000, Photon Beard, UK). Digital video sequences were recorded with a Photron Fastcam SA1 high-speed digital video camera. A Tamron 90-mm camera lens was used at an aperture of f4. Videos were recorded at 10,000 frames per second using exposure times of 2–10 μs.

The second technique was a visualization method known as shadowgraphy, the invention of which has been attributed to Hooke [6–8]. The particular variant of this method used here has become known as Edgerton shadowgraphy [7–9]. This technique utilizes a pseudo-point source of light reflected from a highly reflective surface positioned coaxially to the camera lens (see Fig. 1). An object of interest placed in the light path appears coincident with its magnified shadow on the screen. Small density differences in the fluid medium (air, in this case) can also be visualized with this method. This was advantageous to this study as it enabled ballistic shock waves to be imaged.

A screen was constructed from 1-in.-wide strips of retroreflective tape (Scotchlite™ 7610, 3M Corporation) attached to two 1.22 m high by 0.92 m wide sheet metal targets. One of two different light sources was used for illumination of the screen, either a 400-W xenon arc lamp (Newport-Oriel) or a high-pressure mercury arc lamp (X-Cite 120 fiber-optic light source, EXFO Life Sciences and Industrial Division). A 5-mm diameter rod mirror (Edmund Optics) was mounted onto the center of a standard 28-mm

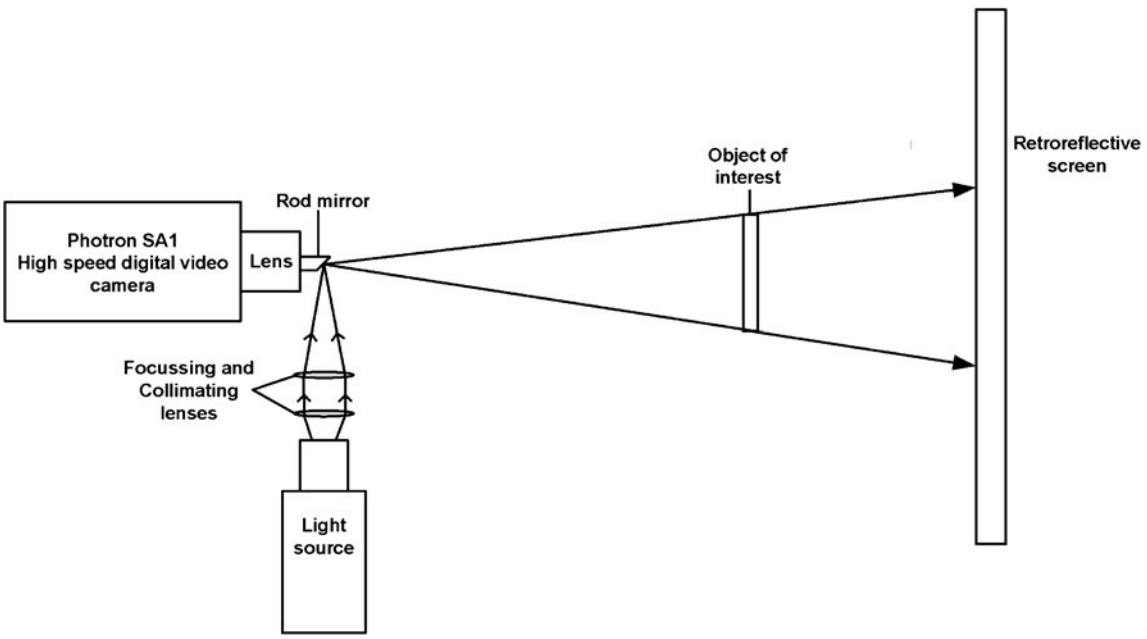

Fig. 1 Diagram of the experimental setup for recording shadowgraphy videos

Nikkor lens filter for wide-angle views (field of view approximately 1 m); a 10-mm diameter rod mirror was mounted onto a 55-mm Nikkor lens filter for close-up shots (field of view approximately 500 mm). The lens aperture was wide open at f2.8 for both configurations. Light from the source lamp was focused onto the rod mirror using a plano-convex lens. Lenses of different focal lengths were used for individual tests, depending on the desired area of illumination. Light reflected off the rod mirror illuminated the retroreflective screen, and the light reflected from the screen was captured using the high-speed camera. For the experimental conditions used in this study, no significant occlusion from the rod mirror on the camera lens filter was observed in the shadowgraphy images.

High-speed shadowgraphy videos were recorded using the Photron Fastcam SA1 camera. The retroreflective screen was placed against one side wall of the firing range, and the light source and camera were positioned near the opposite wall. The firearm was fired in a direction parallel to the screen (toward the front wall of the range), perpendicular to the camera. The flight path of the bullet was located about 92 cm from the screen, at a position corresponding to approximately one third the distance of the total camera-to-screen separation. This was within the range for optimum sensitivity for the shadowgraphy technique [8]. This setup is illustrated in Fig. 2.

A 6-mm-thick sponge, liberally soaked in fresh human blood mixed with EDTA anti-coagulant, was used as the blood source in part 2 of this study. An individual shot was fired into the blood-soaked sponge at distances ranging from near contact to 244 cm (8 ft). In some experiments, two large cardboard targets were also suspended in the bullet's flight path, one 30 cm in front of and the other 30 cm behind the sponge.

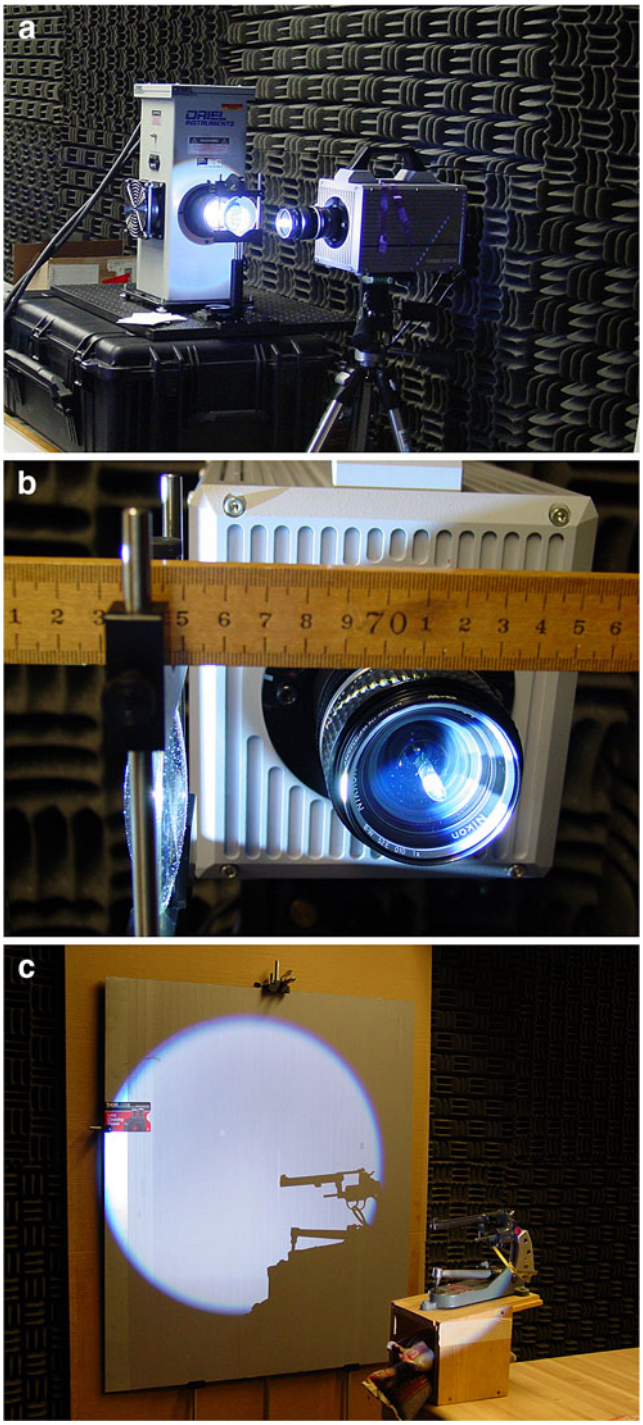

Fig. 2 Photographs of the equipment used for shadowgraphy experiments. **a** Four hundred-Watt xenon arc light source and Photron Fastcam SA1 camera. **b** Five-mm diameter rod mirror mounted onto a Nikkor 28-mm filter. **c** Shadowgraph of a .22 caliber revolver (unloaded chamber) on a retroreflective screen

Results

Part 1: characterizing the discharge of selected firearm/ammunition combinations using Edgerton shadowgraphy

Because of its sensitivity to small fluid density differences, the shadowgraphy technique can be used to monitor ballistic shock waves generated during the discharge of a firearm. The technique was also found to be very effective in visualizing gases and particulate matter that are produced when a firearm is discharged.

This can be seen in Fig. 3 which shows selected images of the discharge of the .38 caliber revolver. Shock waves developed initially at the chamber and muzzle, with a small amount of associated gas discharge. Less than a millisecond later, a subsequent shock wave and significantly more gases and particulate material were produced, coincident with the emergence of the bullet from the muzzle. The muzzle velocity of this ammunition is stated by the manufacturer to be 247 m/s. As a result, it is a subsonic projectile and the ballistic shock wave travels ahead of the bullet, as shown in Fig. 3 (especially Fig. 3f).

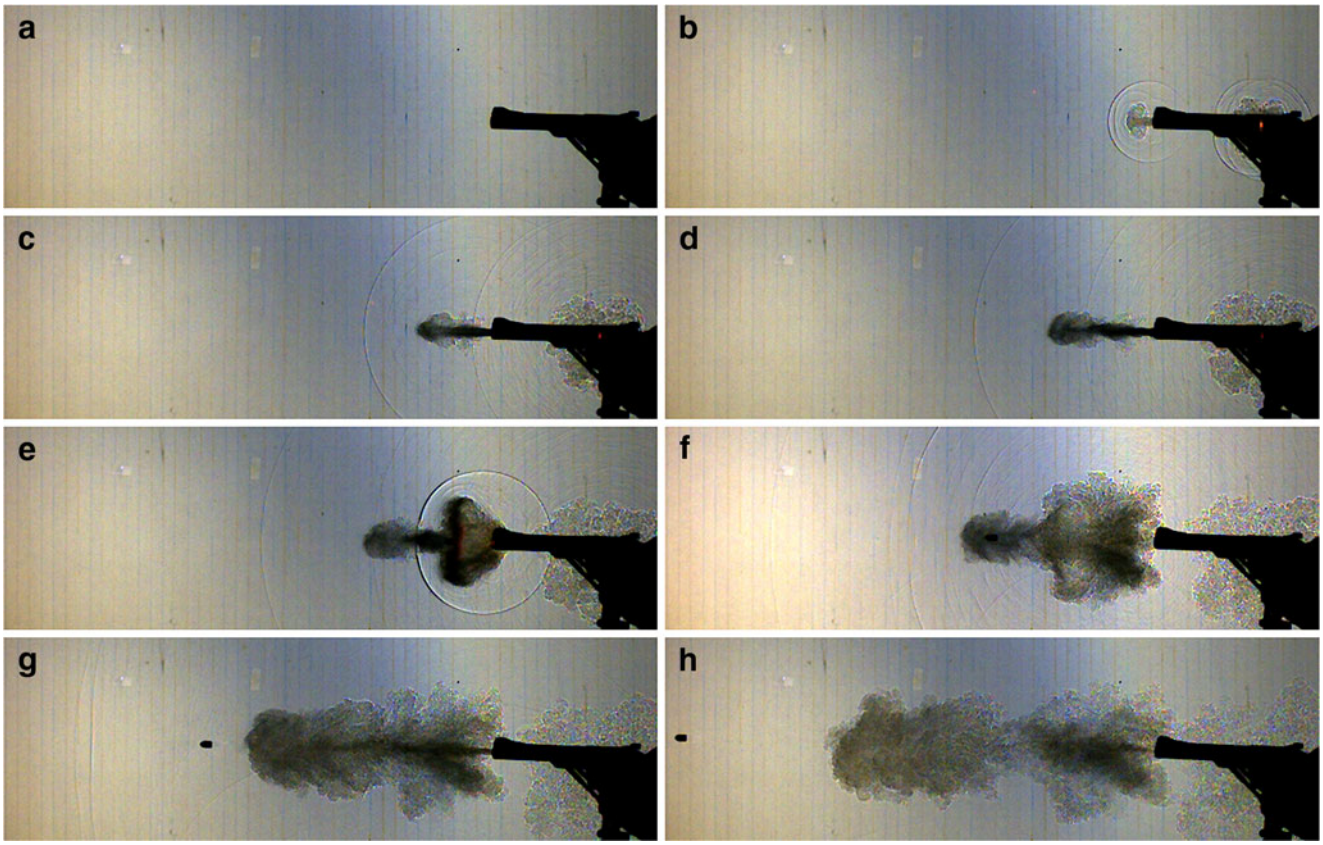

Fig. 3 A sequence of images of the discharge of the .38 caliber revolver. **a** t=0. **b** t=0.3 ms. Shock waves develop at the chamber and muzzle, with associated gases. **c** t=0.6 ms. **d** t=0.8 ms. Third shock wave develops at the muzzle as the bullet emerges. **e** t=1.0 ms. **f** t=1.6 ms. **g** t=2.2 ms. Shock wave travels ahead of the subsonic bullet, followed by muzzle gases. **h** t=3.1 ms

Figure 4 shows selected images of the discharge of the .308 Winchester caliber rifle. Like the .38 caliber revolver, a shock wave was produced at the muzzle, along with the discharge of gases during and following the emergence of the bullet. The bullet velocity for this ammunition is significantly higher (stated by the manufacturer to be 860 m/s), which makes it a supersonic projectile. This is confirmed in Fig. 4 where the bullet can be seen overtaking the ballistic shock wave (see Fig. 4c, d). The supersonic bullet created its own shock wave (the expected V-shape in the images shown), and some turbulence in the flight path of the bullet, along the axis of fired shot, was observed.

Part 2: backspattering of blood from ballistic impact

Figure 5 shows selected images from the recorded high-speed video of a .22 Long Rifle caliber bullet striking a blood source, creating forward spatter and backspatter. In this experiment, which is typical of those used by instructors to demonstrate the phenomenon of backspatter, cardboard targets were positioned between the firearm and blood source and beyond the blood source to collect backspattered and forward-spattered blood, respectively. The cardboard targets are not shown in these images. The characteristic cone-shaped dispersion of blood can be seen after the bullet impacts the sponge.

Figure 6 shows selected images of a .22 Long Rifle caliber bullet striking a bloodied sponge, mounted on cardboard at approximately 45°. This bullet was fired from a distance of 50 cm using the .22 caliber revolver. No intermediate target was used in this experiment. It is notable that the ensuing spatter is initially projected approximately normal to the surface of the sponge; this is shown most clearly in Fig. 6c. This confirms observations made by Bevel and Gardner [1]. Of more interest and potentially greater ramification for forensic investigators is the subsequent interaction observed between the cloud of gases and particulate matter that emanated from the firearm and the spattered, airborne blood droplets. These gases traveled behind the bullet, arrived at the sponge a few milliseconds later, and proceeded to have a dramatic and significant interaction with the blood droplets. Most of the droplets were effectively swept forward, above, and subsequently past the sponge (see Fig. 6e, f).

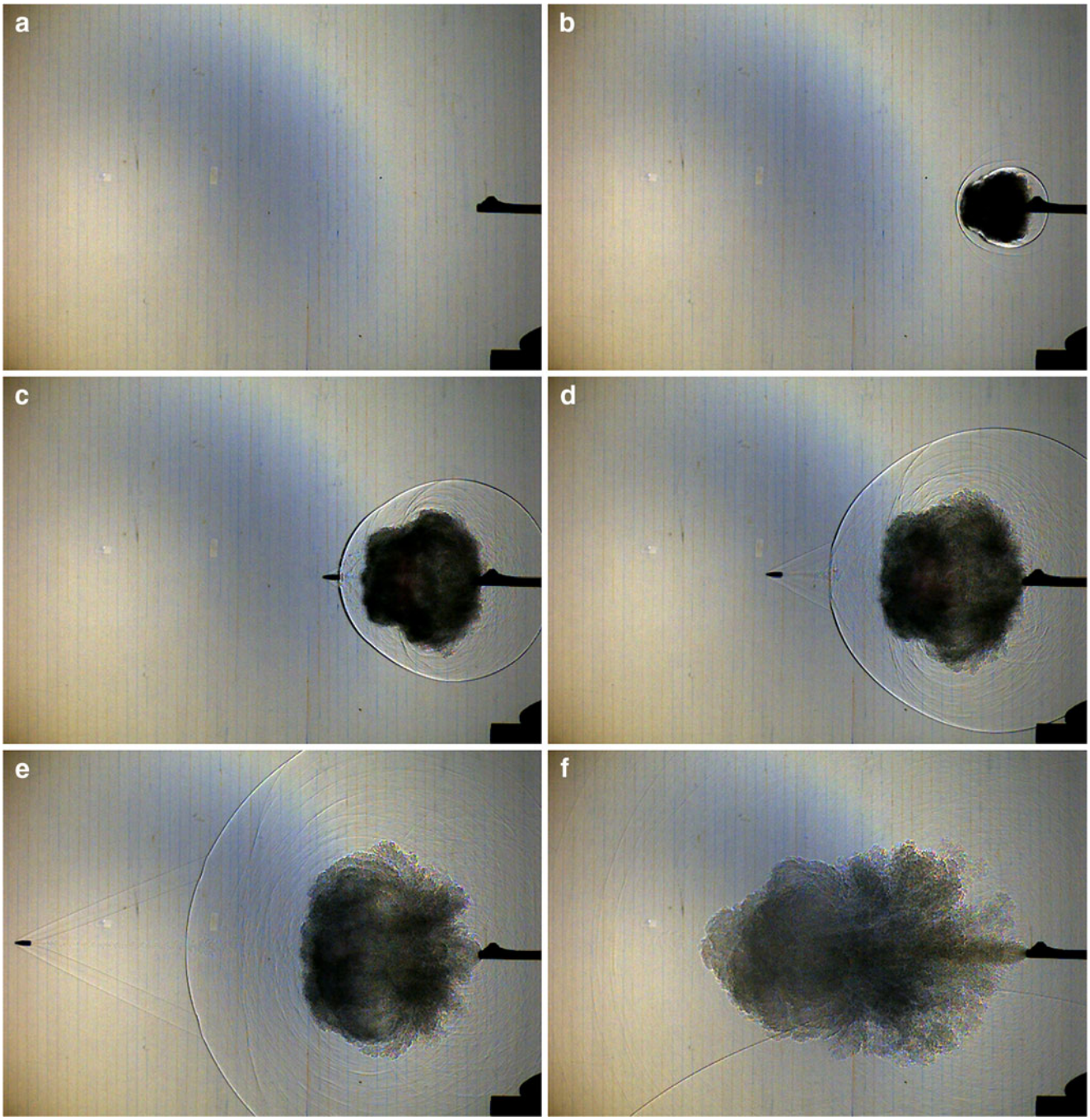

Fig. 4 A sequence of images of the discharge of the .308 Winchester caliber rifle. **a** t=0. **b** t=0.3 ms. Shock wave develops at the muzzle as the bullet emerges, along with gases and particulate matter. **c** t=0.5 ms. **d** t=0.7 ms. Bullet overtakes the ballistic shock wave, creating its own wave and flight path turbulence. **e** t=1.1 ms. Supersonic bullet travels ahead of its ballistic shock wave and muzzle gases. **f** t=2.4 ms. A reflection of the shock wave from an underlying surface

Figure 7 is a photograph of the blood spatter on the cardboard mount, above and behind the impact site on the sponge, for the Fig. 6 experiment. This spatter was blown forward to this location by the gases resulting from the firing of the weapon after the impact from the bullet had initiated some backspattering of blood.

To further investigate the role of muzzle gases and to consider the possible role of ballistic shock waves on airborne blood droplets, backspatter shadowgraphy imaging experiments were conducted.

Figure 8 shows a sequence of selected images of the impact of a .38 caliber bullet striking a bloodied sponge,

Fig. 5 Sequence of images of the impact of a .22 caliber bullet that has passed through an intermediate target (not shown) before striking a bloodied sponge. **a** $t=-0.1$ ms. **b** $t=0$. Impact of the bullet with the blood-soaked sponge. **c** $t=0.1$ ms. **d** $t=0.2$ ms. Characteristic cone-shaped blood spatter observed after impact, in forward and backward directions. **e** $t=0.4$ ms. **f** $t=1.6$ ms

with no intermediate target placed between the revolver and the sponge. For this test, the distance between the muzzle and the sponge was 45 cm. Significant interaction between the gases from the firearm and the spattered blood droplets is evident (see Fig. 8d–f). Many of the original back-spattered droplets are blown forward, toward the surface from which they originated, as the gases begin to interact with the expanding backspatter.

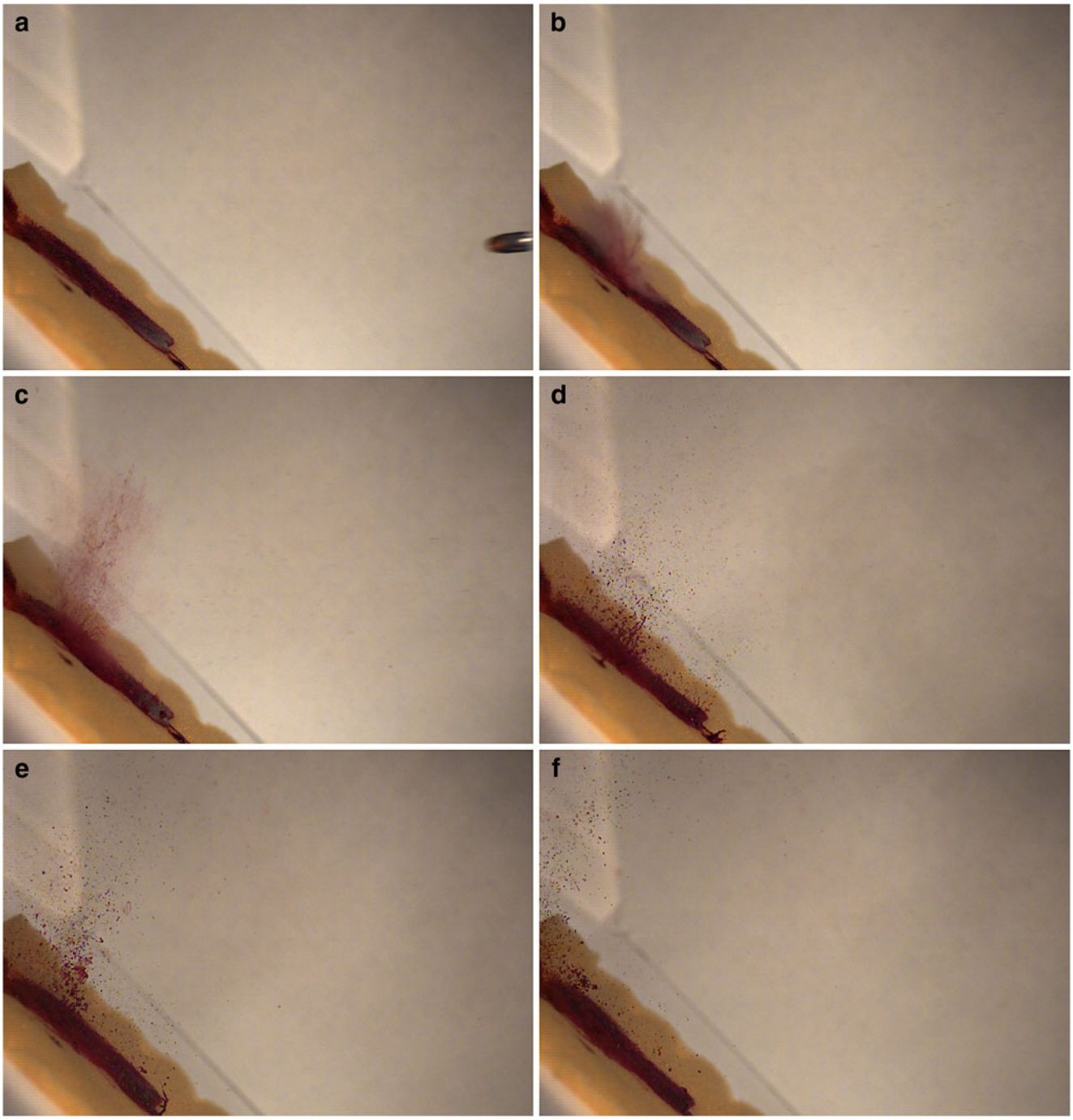

Fig. 6 A sequence of images of the impact of a .22 caliber bullet striking a bloodied sponge at 45° (firearm to blood source distance = 50 cm). **a** $t=-0.4$ ms. Bullet fired at blood-soaked sponge. **b** $t=0$. Bullet strikes sponge surface. **c** $t=0.4$ ms. Blood backspatter, perpendicular to the surface of the sponge. **d** $t=3.3$ ms. Gases arrive and begin interacting with the droplet cloud. **e** $t=7.4$ ms. Blood spatter blown forward by the muzzle gases. **f** $t=9.8$ ms

Figure 9 shows a sequence of selected images of the impact of a .308 Winchester bullet striking a bloodied sponge, with no intermediate target placed between the rifle and the sponge. For this test, the rifle-to-sponge distance was 45 cm. Again, significant interaction is observed between spattered blood droplets and the gases from the weapon. For this firearm and ammunition, a larger quantity of gas at higher pressure was produced, which was even more effective in changing the trajectories of the spattered blood droplets. Rather violent interaction of the gases with the blood droplets occurred (see Fig. 9d–f). In additional images not shown in Fig. 9, the pressurized gases were

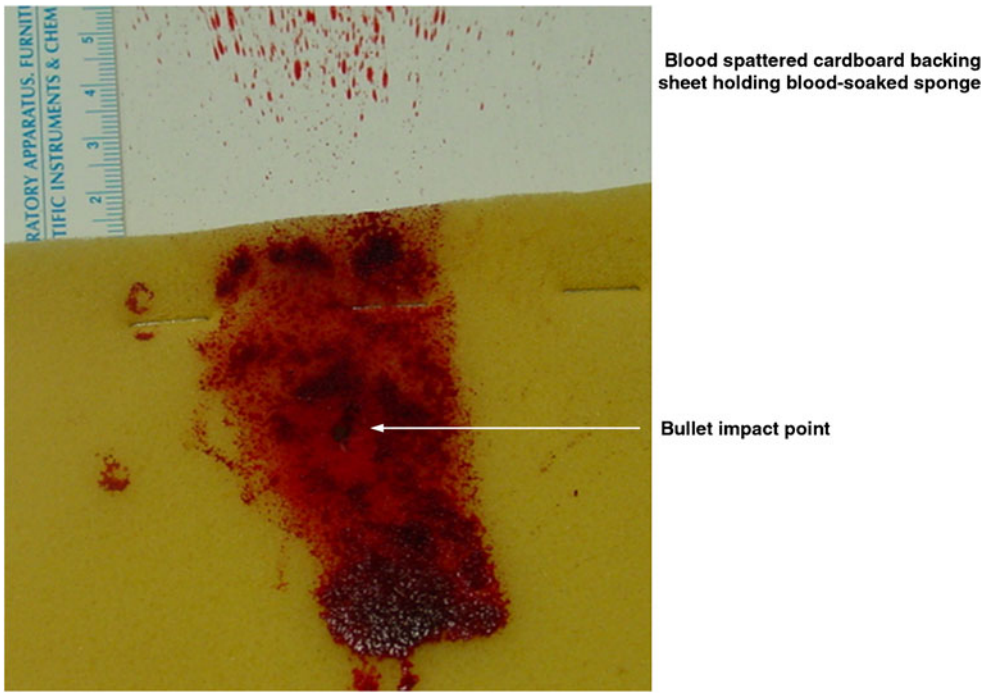

Fig. 7 Photograph of blood spatter observed for the experiment shown in Fig. 6. Blood droplets have been blown forward and to the sides of the original blood source

observed to cause movement of the cardboard around the sponge, as well as metal binder clips attached to the support target.

Figure 10 shows a sequence of selected images of the impact of a .22 caliber bullet passing through an intermediate target before striking a bloodied sponge. For this test, the distance from the gun to the sponge was 87 cm, with the intermediate target positioned 30 cm from the sponge. The blocking effect of the intermediate target and its impact on the lack of interaction of the gases with the backspattered blood droplets are plain to see. The gases are effectively blocked (see Fig. 10c, d) until they begin to dissipate (Fig. 10e, f). As a result, only very limited interaction of small pieces of the intermediate target and a very small fraction of the gases generated by the firing of the gun occurs with the blood droplets. Obvious backspatter was observed on the surface of the intermediate target in this experiment.

For both the subsonic (.22 and .38) and the supersonic (.308) bullets used in these experiments, including the results for numerous other high-speed shadowgraphy videos not shown here, no discernable interaction between the ballistic shock waves and backspattered blood droplets was observed.

Conclusions

The experiments described in this study have demonstrated that the muzzle gases produced by the discharge of a firearm can play a significant role in the spattering of blood, thereby affecting the patterns of backspatter observed. It is acknowledged that a bloodstained sponge is not a realistic model for producing blood spatter associated with a single gunshot wound. Perhaps at best it might reproduce some of the characteristics of injuries from multiple shots. However, the results presented from this study clearly indicate that any bloodstain pattern produced by backspatter from a gunshot wound could well be influenced by the muzzle gases generated from the firearm discharge.

The implications of the air–blood interaction described in this work are significant for those expressing

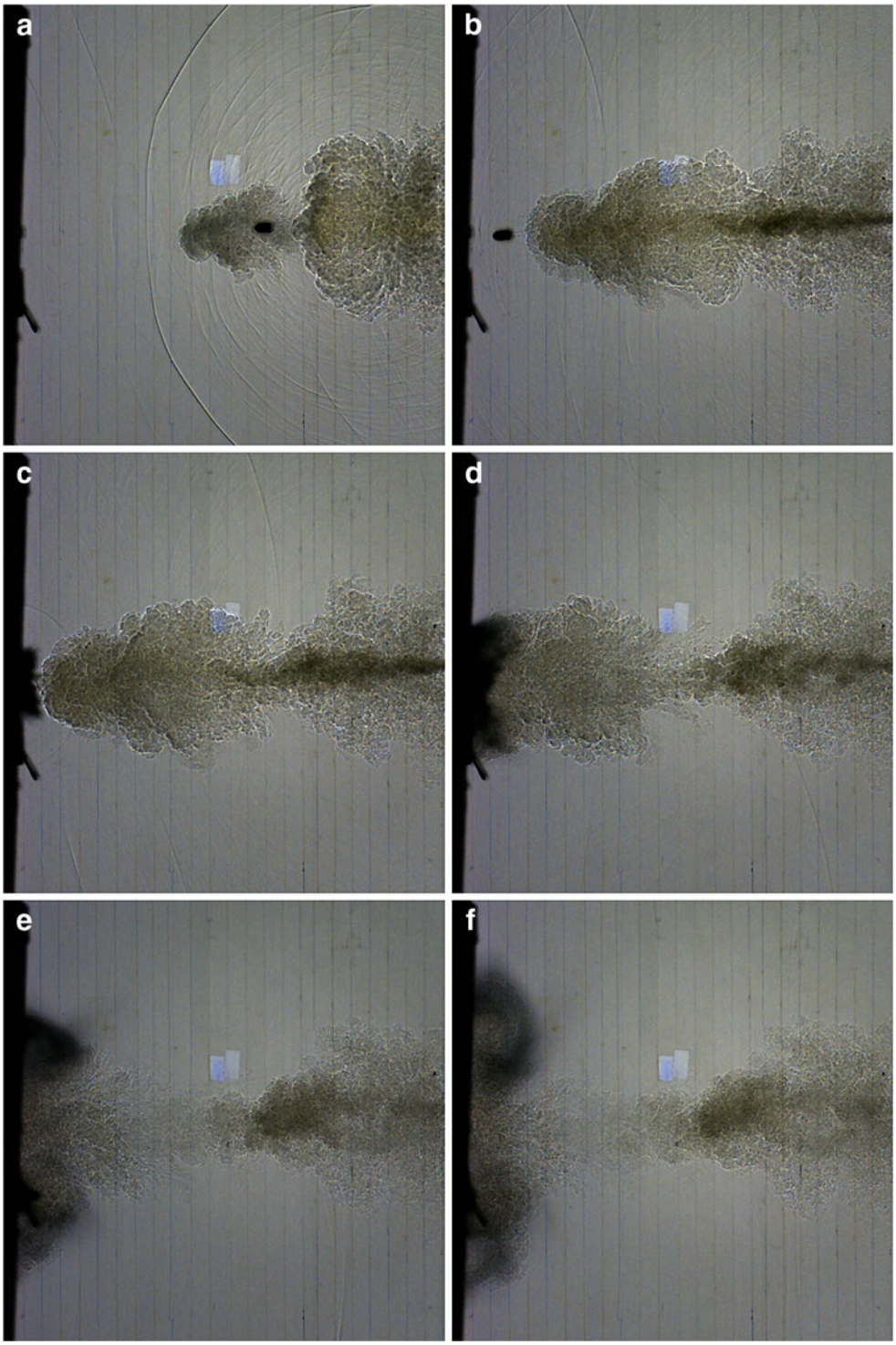

Fig. 8 Sequence of images of the impact of a .38 caliber bullet striking a bloodied sponge (firearm to blood source distance= 45 cm; no intermediate target). **a** $t=-1.0$ ms. Subsonic bullet and gases emerging from barrel, along with ballistic shock waves. **b** $t=-0.3$ ms. Bullet approaches the blood source, followed by muzzle gases. **c** $t=0$. Bullet strikes the blood source initiating backspatter of blood prior to gases arriving. **d** $t=0.5$ ms. Muzzle gases interact with the dispersing backspatter. **e** $t=1.6$ ms. Gases set up an interaction with backspattered blood droplets. **f** $t=2.4$ ms. Turbulent gas flow causes many drops to be forced forward toward their origin

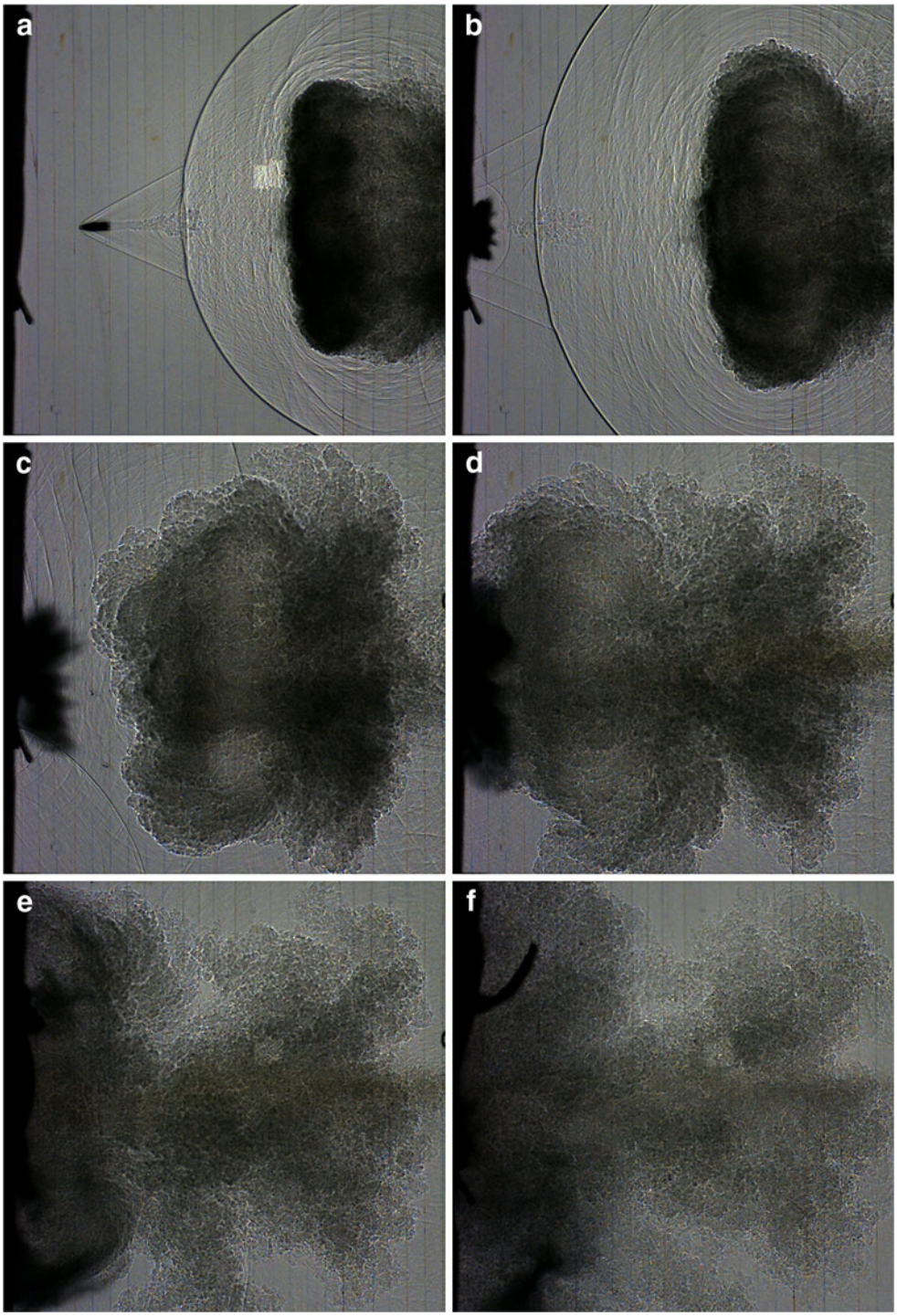

Fig. 9 Sequence of images of the impact of a .308 Winchester caliber bullet striking a bloodied sponge (firearm to blood source distance=45 cm; no intermediate target). **a** $t=-0.2$ ms. Supersonic bullet and gases emerging from barrel, along with ballistic shock waves. **b** $t=0$. Bullet strikes the blood source, initiating backspatter. **c** $t=0.8$ ms. Backspatter disperses ahead of approaching muzzle gases. **d** $t=1.4$ ms. Gases begin to interact with backspatter. **e** $t=2.2$ ms. Gases set up an interaction with backspattered blood droplets. **f** $t=4.2$ ms. Violent dispersion of blood droplets occurs near the target

an expert opinion on backspatter in criminal trials. In particular, great care should be taken in attaching significance to the absence of backspatter on an accused person or a firearm. In addition to the possibility that the shooter was not in close proximity, an absence of backspatter could be the result of the sweeping effect of air currents from the discharge of the firearm, effectively shielding the accused and the firearm from the blood backspatter. It is possible that the air–blood interaction could be evidenced by the presence of spattered stains around the perimeter of a gunshot wound, with a component of directionality the same as the direction of the bullet.

Instructors of bloodstain pattern courses need to be mindful that experiments that use intermediate targets to show backspatter suffer from the limitation of eliminating the air–blood interaction that is likely to be significant for close-range shots.

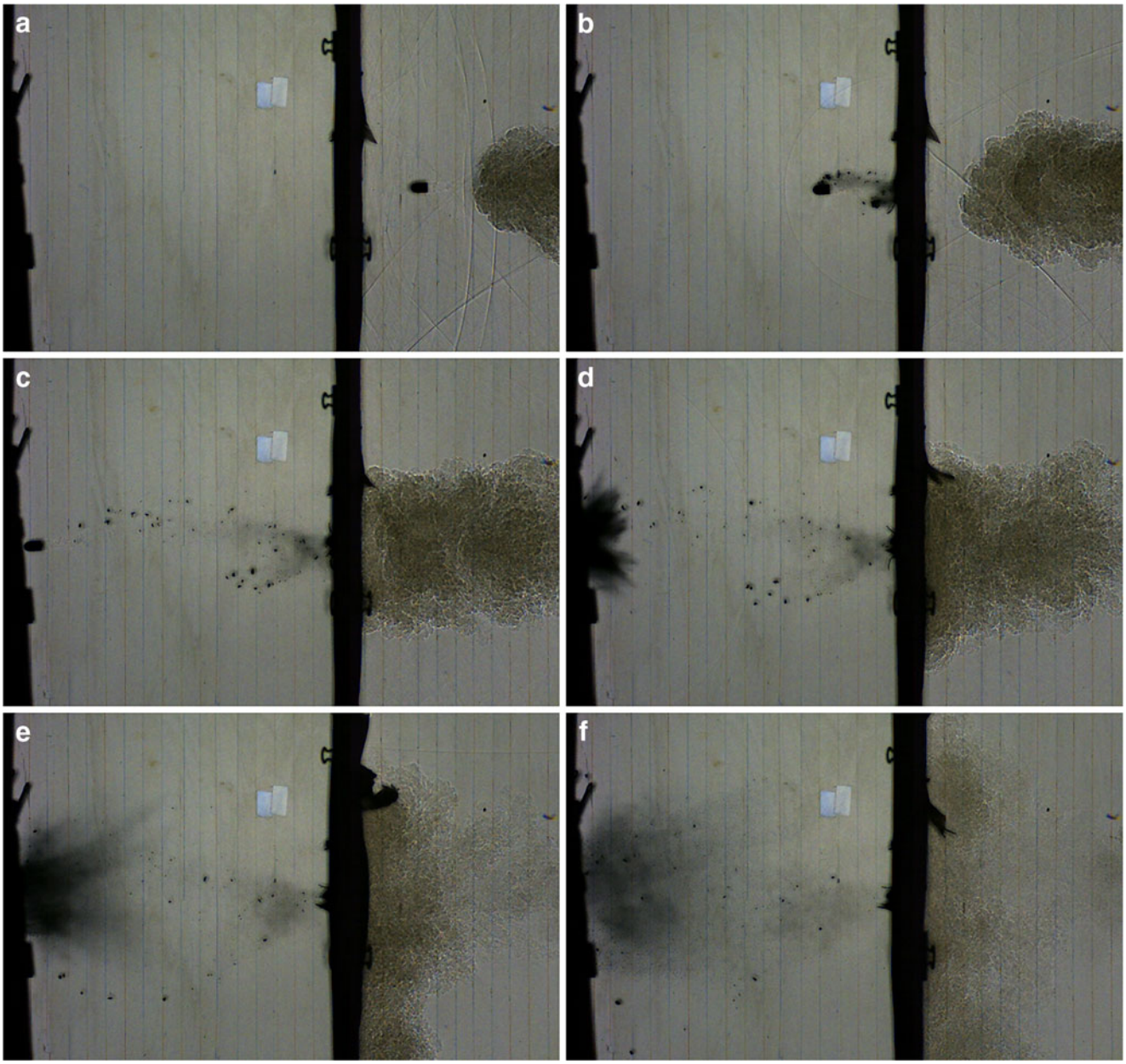

Fig. 10 Sequence of images of the impact of a .22 caliber bullet passing through an intermediate target before striking a bloodied sponge (firearm to blood source distance=87 cm, intermediate target to blood source distance=30 cm). **a** $t=-1.2$ ms. Bullet approaches the intermediate target, followed by muzzle gases. **b** $t=-0.7$ ms. Bullet passes through the intermediate target. **c** $t=0$. Bullet about to strike the blood source, while gases strike the intermediate target. **d** $t=0.5$ ms. Bullet passes through the blood source initiating backspatter, while the gases are blocked by the intermediate target. **e** $t=2.9$ ms. Blood continues to spatter while the gases dissipate behind the intermediate target. **f** $t=8.8$ ms

The extent of the air–blood interaction is expected to be a function of the firearm–ammunition combination used, as well as the firing distance. This will be the subject of a further study.

Acknowledgments This study was supported by a National Institute of Justice grant administered by the Midwest Forensics Resource Center, Ames Laboratory-USDOE (Interagency Agreement #2008-DN-R-038), as well as Crown Research Institute Capability Funds from the Institute of Environmental Science and Research (ESR), New Zealand, Ltd. Ames Laboratory is operated for the US Department of Energy by Iowa State University under contract no. DE-AC02-07CH11358. The authors would like to acknowledge the willing support offered by the Minnesota Bureau of Criminal Apprehension, in particular Mr. Kurt Moline and Mr. Eldon Ukestad of the firearms section, as well as Mr. Kevan Walsh, ESR, Auckland, for his helpful comments during the preparation of the manuscript.

Ethical standards All experiments referred to in this manuscript comply with the current laws of the United States of America and of New Zealand.

Conflict of interest The authors declare that they have no conflict of interest.

References

1. Bevel T, Gardner RM (2008) Bloodstain pattern analysis: with an introduction to crime scene reconstruction, 3rd edn. CRC, Boca Raton
2. James SH, Kish PE, Sutton TP (2005) Principles of bloodstain pattern analysis: theory and practice. CRC, Boca Raton
3. Karger B, Nüsse R, Brinkmann B, Schroeder G, Wüstenbecker S (1996) Backspatter from experimental close-range shots to the head. I. Macrobackspatter. Int J Leg Med 109:66–74
4. Laber TL, Epstein BP (1983) Experiments and practical exercises in bloodstain pattern analysis, 4th edn. Callan, Minneapolis
5. Laber TL, Epstein BP, Taylor MC (2008) High speed digital video analysis of bloodstain pattern formation from common bloodletting mechanisms. IABPA News 2008 (June), pp 4–12
6. Hooke R (1677) Lampas. J. Martyn, London
7. Settles G S, Grumstrup T P, Miller J D, Hargather MJ, Dodson LJ, Gatto J A (2005) Full-scale high-speed "Edgerton" retroreflective shadowgraphy of explosions and gunshots. Proceedings of 5th Pacific Symposium on Flow Visualization and Image Processing, Australia
8. Settles GS (2001) Schlieren and shadowgraph techniques: visualizing phenomena in transparent media. Springer, Berlin
9. Edgerton HE (1958) Shock wave photography of large subjects in daylight. Rev Sci Instrum 29(2):171–172